

ABSTRACT

Background Most patients with solid malignancies harbor innate or acquired resistance to immune checkpoint blockade (ICB), prompting the need for novel therapeutic strategies. Interleukin-12 (IL-12) is a promising cytokine for cancer therapy due to its ability to bridge innate and adaptive immunity. However, a narrow therapeutic index limits the use of systemic IL-12 therapy. Here, we investigated the tumor-suppressive effects and mode of action of intratumorally delivered murine Interleukin-12 anchored to aluminum hydroxide (referred as mANK-101)^{1,2} in combination with the class I HDAC inhibitor Entinostat, in various ICB-refractory murine tumor models, including CT26 (colorectal) and MOC-1 (HPV16^{neB}). We hypothesized that combining Entinostat with an anchored form of IL-12 could overcome systemic toxicity while maintaining anti-tumor activity.

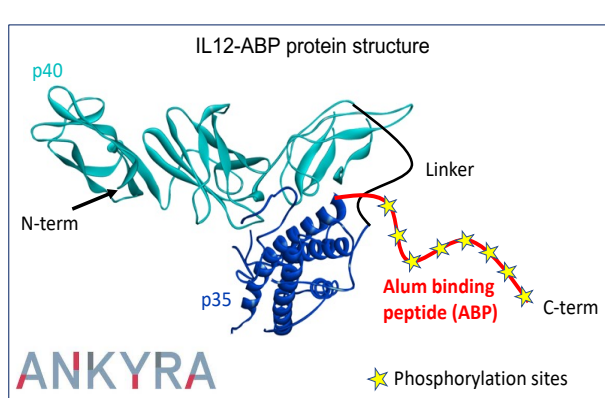
Methods Entinostat and intra-tumoral mANK-101 were administered to mice bearing well-established αPD1-refractory CT26 (colorectal) and MOC-1 (HPV16^{neB}) tumors. Antitumor activity, survival, and protective memory upon tumor rechallenge were evaluated. Comprehensive proteomic and immune cell analysis was performed in MOC-1 tumors, tumor-draining lymph node (tdLN), and periphery. Tumor-specific T cell responses were examined.

Results We demonstrate that intra-tumoral mANK-101 synergizes with Entinostat to suppress multiple αPD1-refractory tumors, resulting in significant tumor eradication (62-88%), survival benefit (P < 0.0001), and protective memory, including CT26 (colon, Kras G12D^{mut}) and MOC-1 (oral, HPV16^{neB}). Analysis of MOC-1 tumor-bearing mice demonstrated these effects to be associated with peripheral activation of CD8⁺ and NK lymphocytes, augmented polyfunctional IFNγ/TNFα⁺-producing CD8⁺ T cells, CD8⁺ T cell effector memory, and tumor-specific T cell responses. Significant decrease in CD4⁺ Tregs and increased CD8/Treg ratio were also observed. Ongoing functional studies, proteomic and immune cell analysis at the tumor site, tdLN, and periphery, including single cell transcriptomics and epigenetic studies, will allow for a deeper understanding of the synergistic effect of mANK-101 with the epigenetic modulator Entinostat.

Conclusions Collectively, these findings form a rationale for the clinical combination of intralesional delivery of ANK-101 with Entinostat for patients with ICB-refractory malignancies, including colorectal and HPV16^{neB} head and neck cancers.

MATERIALS AND METHODS

Reagents. mANK-101 and Entinostat were kindly provided by Ankyra Therapeutics and Syndax under Cooperative Research and Development Agreements (CRADA), respectively. Entinostat was formulated into a low-fat diet of 35% sucrose for a target daily dose of 6mg/kg (Research Diets).



Tumor studies and treatments (in brief). MOC-1 and CT26 tumor cells were implanted subcutaneously (s.c.) into the right or the left flank of C57Bl/6 (MOC-1) or Balb/c (CT26) mice for respective studies. Mice were randomized to receive Entinostat (p.o.) or intra-tumoral (i.t.) injections of mANK-101 as depicted in designated Figures. A sub-optimal dose of ANK-101 (2ug) has been chosen to explore the combination potential of ANK-101 with Entinostat. Analysis of spleen and tumor immunomes was performed by flow cytometry. Cytokines and chemokine proteins were examined in the TME and sera.

Statistics. One-way ANOVA with Tukey's multiple comparisons were used for data presented in violin plots. Two-way ANOVA was used to analyze tumor growth curves. Survival was analyzed using Log-rank (Mantel-Cox) test. All tumor growth data are representative of 2 independent experiments. Statistical significance was set at *p < 0.05, **p < 0.005, ***p < 0.001.

RESULTS

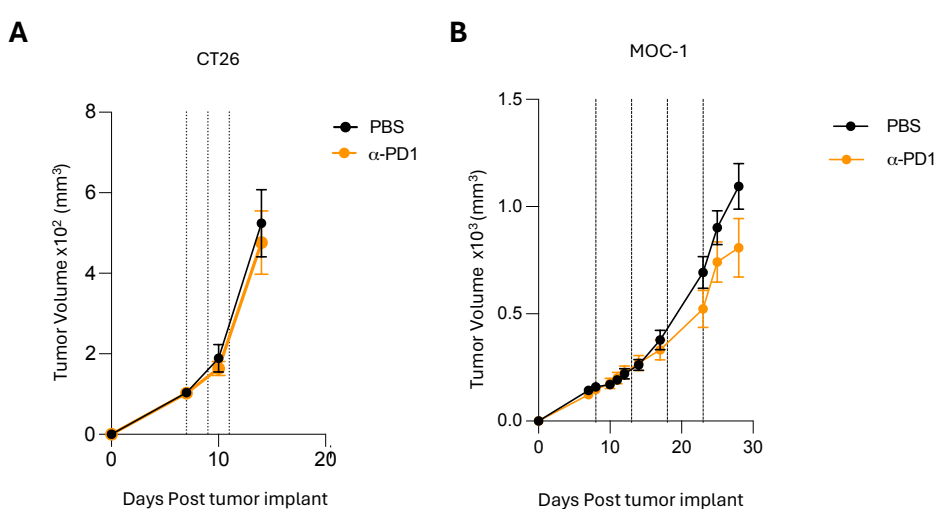


Figure 1. Response of CT26 and MOC-1 tumor models to immune checkpoint blockade. Respective aggregate tumor growth curves for CT26 (A) and MOC-1 (B) for PBS and anti-PD1 treatment groups.

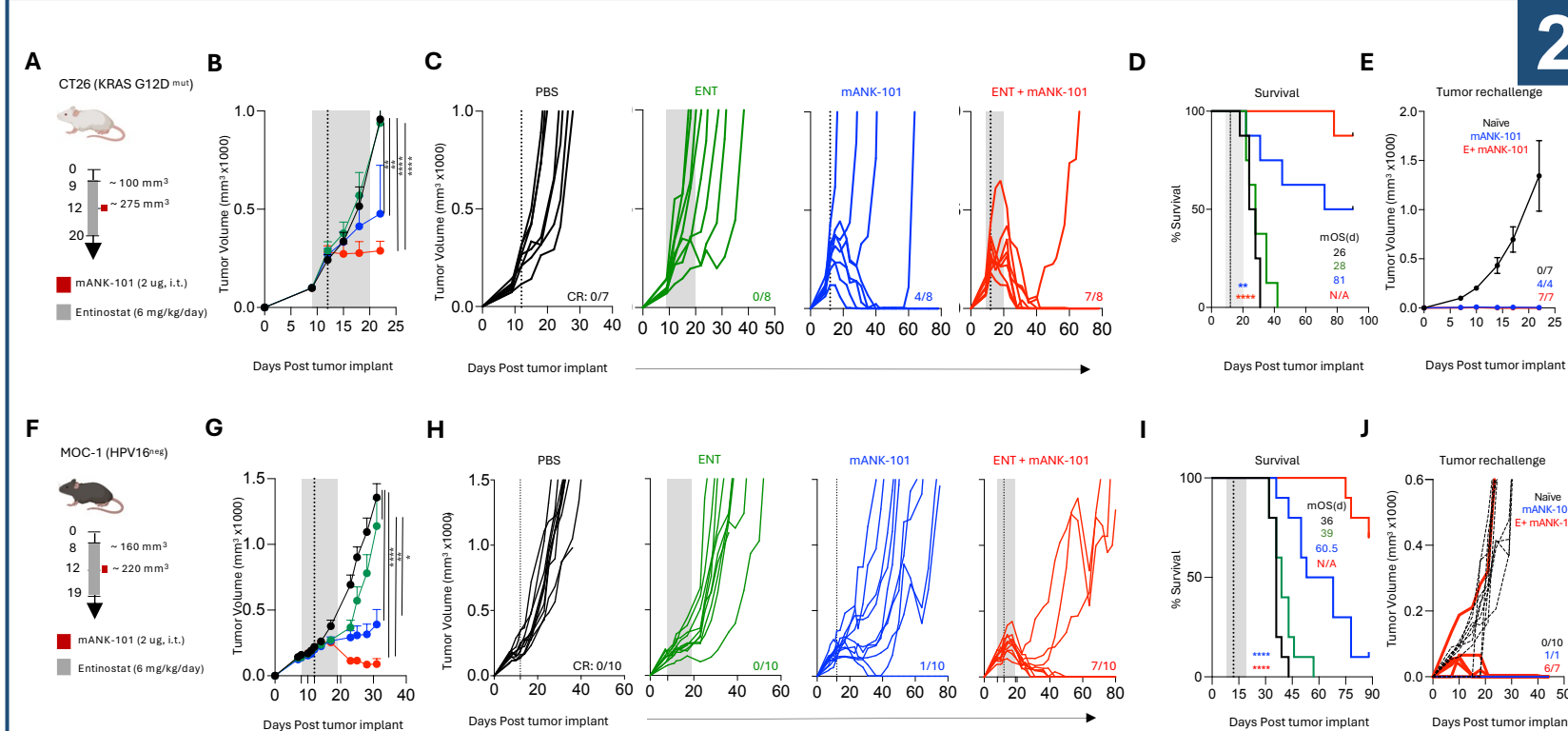


Figure 2. mANK-101 synergizes with Entinostat to suppress CT26 and MOC-1 tumors, eliciting protective memory and increasing survival. Study schematic for (A) CT26 and (F) MOC-1 tumor models. Respective aggregate (B, G) and individual tumor growth curves with cure rates (CR) (C, H) for each treatment group. (D, I) Graphs displays % survival and median overall survival (mOS) for tumor-bearing mice. Graphs show tumor growth curves of naïve or CT26 (E) and MOC-1 (J) cured mice rechallenged with matching tumor cells. Dotted lines: mANK-101 dosing; grey bar: Entinostat diet.

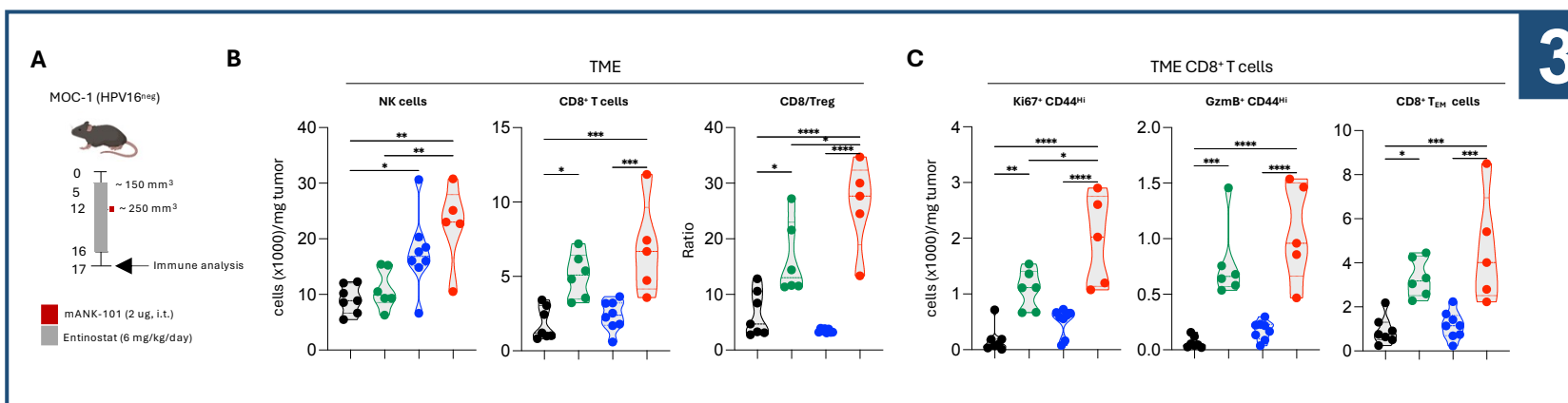


Figure 3. Entinostat and mANK-101 combination induces a pro-inflammatory environment in the TME. (A) MOC-1 study schematic. (B) Number of NK cells and CD8⁺ T cells per mg of tumor, and ratio of CD8/Treg in the TME. (C) Number of Ki67⁺ CD44^{hi} CD8⁺ T cells, Granzyme B⁺ (Gzmb⁺) CD44^{hi} CD8⁺ T cells, and CD8⁺ T_{EM} cells per mg of tumor. (D) MHC-I gMFI of H-2D^p in CD45 negative cells in the TME. Heat maps of tumor chemokine (E) and cytokine (F) proteins as fold-change versus untreated control.

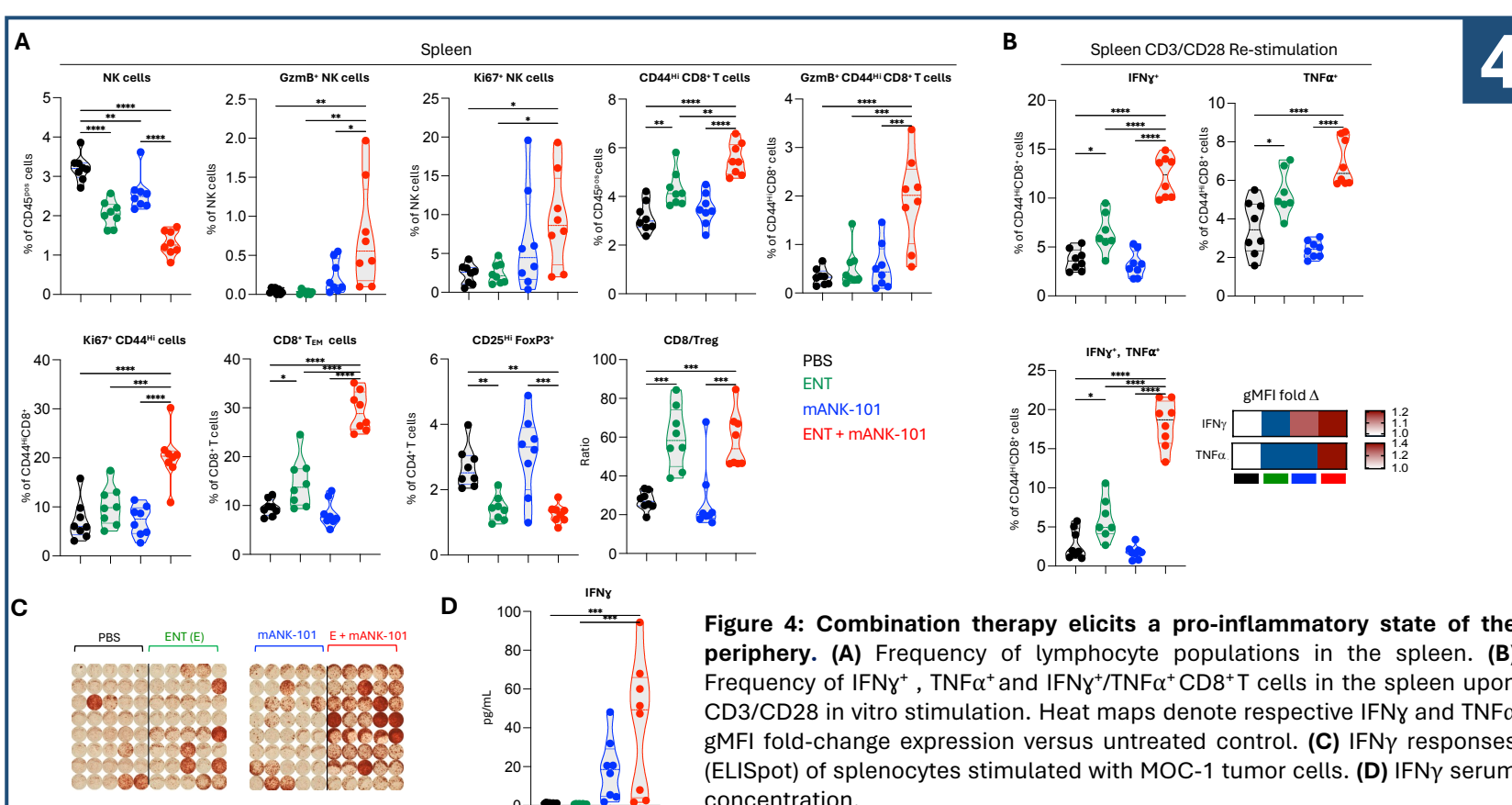


Figure 4: Combination therapy elicits a pro-inflammatory state of the periphery. (A) Frequency of lymphocyte populations in the spleen. (B) Frequency of IFNγ⁺, TNFα⁺ and IFNγ⁺/TNFα⁺ CD8⁺ T cells in the spleen upon CD3/CD28 in vitro stimulation. Heat maps denote respective IFNγ and TNFα gMFI fold-change expression versus untreated control. (C) IFNγ responses (ELISpot) of splenocytes stimulated with MOC-1 tumor cells. (D) IFNγ serum concentration.

RESULTS

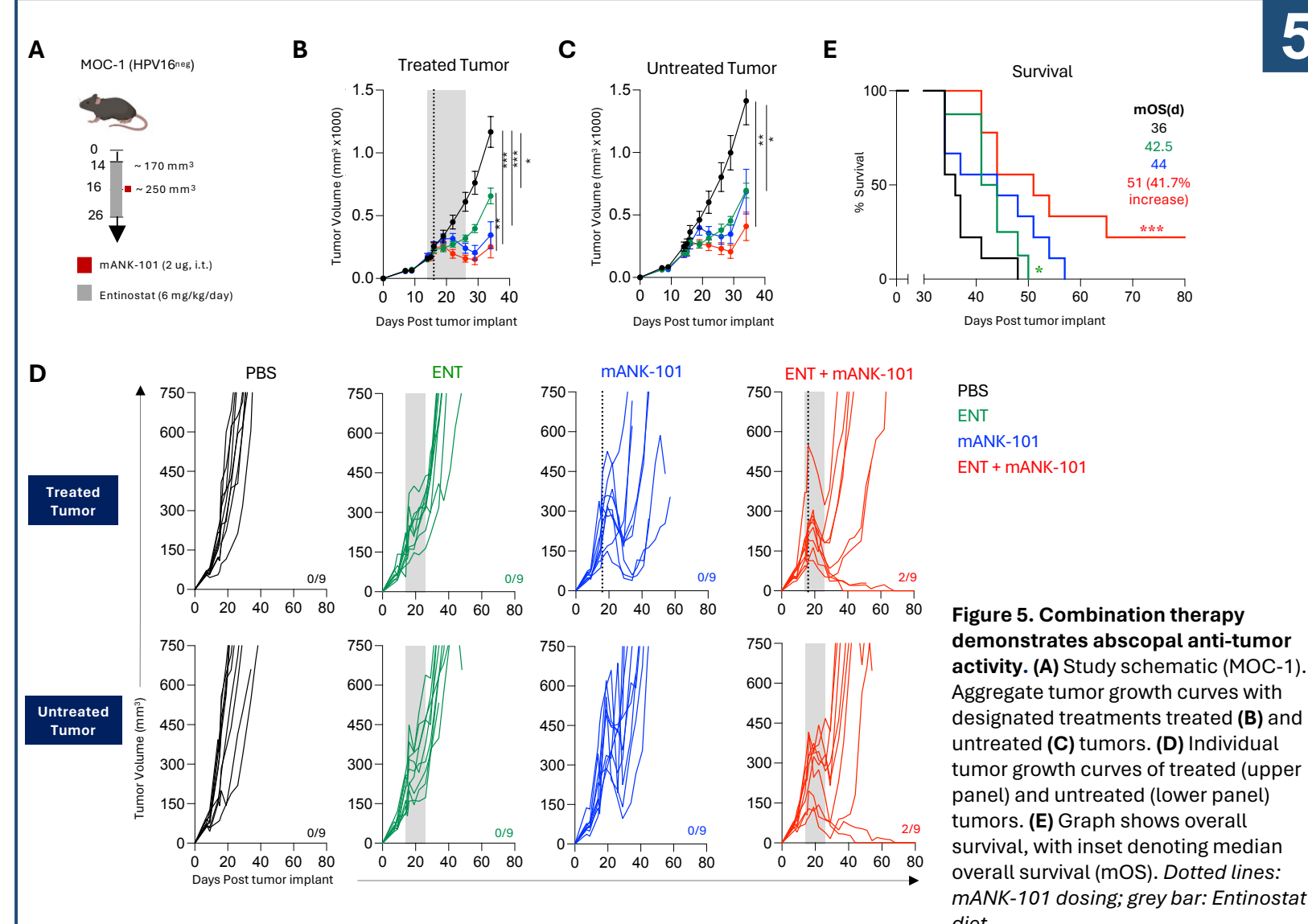


Figure 5. Combination therapy demonstrates abscopal anti-tumor activity. (A) Study schematic (MOC-1). Aggregate tumor growth curves with designated treatments (B) and untreated (C) tumors. (D) Individual tumor growth curves of treated (upper panel) and untreated (lower panel) tumors. (E) Graph shows overall survival, with inset denoting median overall survival (mOS). Dotted lines: mANK-101 dosing; grey bar: Entinostat diet.

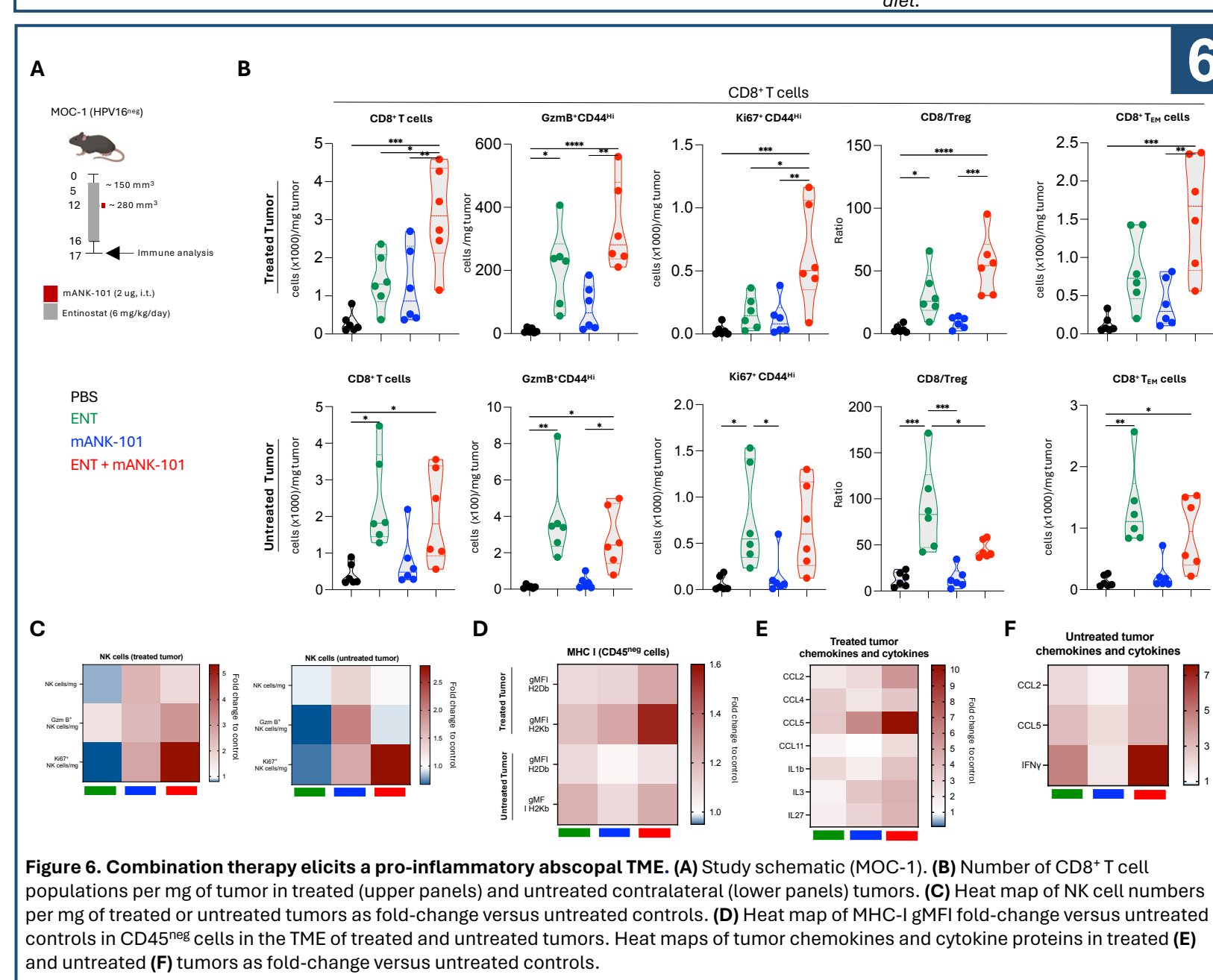


Figure 6. Combination therapy elicits a pro-inflammatory abscopal TME. (A) Study schematic (MOC-1). (B) Number of CD8⁺ T cell populations per mg of tumor in treated (upper panels) and untreated contralateral (lower panels) tumors. (C) Heat map of NK cell numbers per mg of treated or untreated tumors as fold-change versus untreated controls. (D) Heat map of MHC-I gMFI fold-change versus untreated controls in CD45^{neg} cells in the TME of treated and untreated tumors. Heat maps of tumor chemokines and cytokine proteins in treated (E) and untreated (F) tumors as fold-change versus untreated controls.

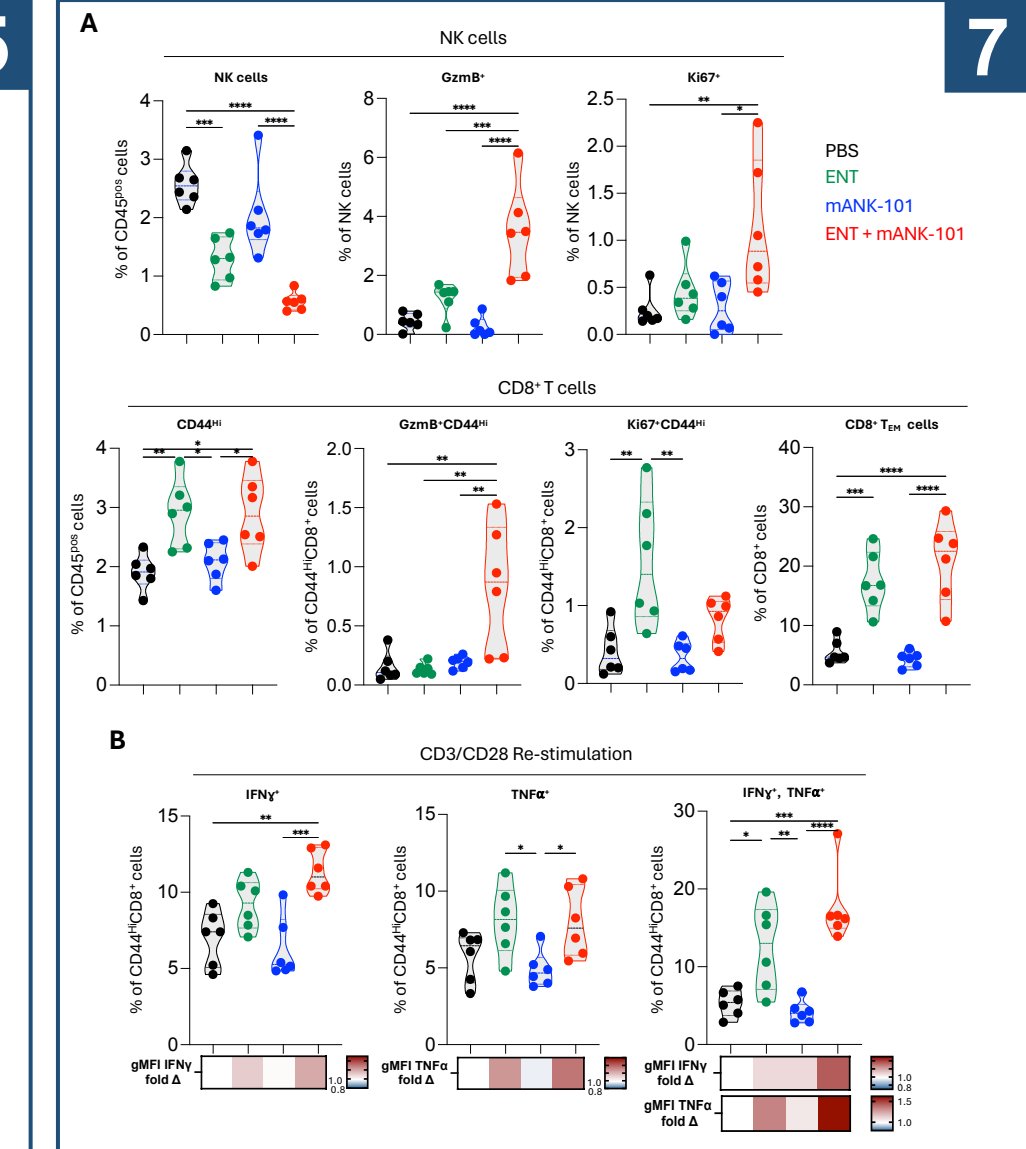


Figure 7. Combination therapy activates lymphocytes in the periphery and promotes CD8⁺ T cell function in the abscopal HPV16^{neB} MOC-1 model. (A) Frequency of lymphocyte populations in the spleen. (B) Frequency of IFNγ⁺, TNFα⁺ and IFNγ⁺/TNFα⁺ CD8⁺ T cells in the spleen upon CD3/CD28 in vitro stimulation. Heat maps denote respective IFNγ and TNFα gMFI fold-change versus untreated control.

SUMMARY

- Combination therapy with mANK-101 and Entinostat synergized to elicit significant anti-tumor effects and prolonged survival in CT26 (colorectal) and MOC-1 (HPV16^{neB}) tumors relative to single agent therapies.
- Tumor suppression was associated with:
 - Increased activation of CD8⁺ T cells in the periphery and the TME.
 - Augmented CD8⁺ T cell function.
 - Increased cytokines and chemokines in the TME.
 - Augmented tumor-specific memory responses.
- Abscopal studies demonstrated tumor suppression of untreated tumors.
- Future proteomic and single-cell transcriptomic investigations will allow for a deeper understanding of the mechanisms by which combination therapy suppresses tumors.
- Collectively, these data support the use of ANK-101 in combination with Entinostat for the treatment of patients with ICB-refractory malignancies, including colorectal and HPV16^{neB} head and neck cancers.

ACKNOWLEDGMENTS

We would like to thank Curtis Randolph and Emily Gonzalez for their exceptional technical assistance on this project.

REFERENCES

1. Battula S. *et al.* Intratumoral aluminum hydroxide-anchored IL-12 drives potent antitumor activity by remodeling the tumor microenvironment. *JCI Insight.* 8(23):e168224, 2023.
2. Agarwal Y. *et al.* Intratumorally injected alum-tethered cytokines elicit potent and safer local and systemic anticancer immunity. *Nature Biomedical Engineering* 6, 129-143 (2022).